Phys. Status Solidi B **248**, No. 9, 2082–2086 (2011) / **DOI** 10.1002/pssb.201147195

physica status solidi b
www.pss-b.com
basic solid state physics

Pentagonal puckering in a sheet of amorphous graphene

Y. Li[1], F. Inam[2], Avishek Kumar[3], M. F. Thorpe[3], and D. A. Drabold[*,1]

[1] Department of Physics and Astronomy, Ohio University, Athens, OH 45701, USA
[2] The Abdus Salam ICTP, Strada Costiera 11, Trieste 34151, Italy
[3] Department of Physics, Arizona State University, Tempe, AZ 85287, USA

Received 8 April 2011, revised 19 June 2011, accepted 21 June 2011
Published online 13 July 2011

Keywords amorphous graphene, density functional theory, fullerenes, puckering

[*] Corresponding author: e-mail drabold@ohio.edu, Phone: +1 740 593 1715, Fax: +1 740 593 0433

Ordered graphene has been extensively studied. In this paper, we undertake a density functional study of *topologically disordered* analogs of graphene, in the form of a random network, consisting predominantly of hexagonal rings, but also including pentagons and heptagons. After some preliminaries with crystalline material, we relax various random network models and find that the presence of carbon pentagons induce local curvature, thus breaking the initial planar symmetry, in some analogy with the case of fullerenes. Using density functional theory to calculate the total energy, we find that while the planar state is locally stable, there is a puckered state that has lower energy. The scale of the puckering is consistent with that expected with local maxima and minima associated with pentagons surrounded by larger rings, forming local "buckyball domes".

1 Introduction Graphene is among the hottest topics in current condensed matter science. A vast amount of work on many aspects of crystalline graphene has appeared. In this paper we take a different tack: we explore the role of topological disorder in amorphous graphene.

The structure of conventional amorphous semiconductors like amorphous Si or Ge is well represented by the continuous random network (CRN) model introduced by Zachariasen [1] nearly 80 years ago. The CRN model has the simplicity that each of the atoms should satisfy its local bonding requirements, and should have minimum strain, characterized by having a narrow bond angle and bond-length distribution. Recently an amorphous graphene CRN model was proposed [2]. Here we develop Kapko et al.'s work [2], and show that pentagons induce curvature in the free standing sheets and analyze the electronic properties.

2 Models To calculate the density of states of crystalline graphene, a 800-atom model (800 c-g) was constructed. For amorphous graphene, we used one 800-atom (800 a-g) model and two 836-atom models (836 a-g1 and 836 a-g2). These amorphous graphene models were all prepared by a modified Wooten–Weaire–Winer (WWW) method [2].

3 Crystalline graphene

3.1 Band structure When calculating the band structure of graphene, tight-binding and *ab initio* methods are two widely used tools. Reich et al. [3] have compared the result of tight binding with *ab initio*. Nowadays, two of the widely used *ab initio* programs are SIESTA [8], using pseudopotentials and the Perdew–Zunger parameterization of the local-density approximation (LDA), and Vienna ab-initio simulation package (VASP) [9], with pseudopotentials, plane-wave basis and LDA.

We computed the eight lowest-energy bands of graphene, by using a single-ζ (SZ) basis set with and without Harris functional, a double-ζ, polarized (DZP) basis set with SIESTA, and also VASP. 20 k-points along each special symmetry line were taken for both SZ and DZP calculations by SIESTA, and 50 k-points points along each line for VASP. The results of SZ and DZP are essentially identical for occupied bands, and exhibit differences for the unoccupied states. Figure 1 shows SIESTA results using SZ basis with Harris functional and VASP. We compared our results with the other first principle calculations [4, 5]. The VASP and SIESTA results are in good agreement with published results for each code [4, 5]. However, as shown in Fig. 1, the calculation based on SZ has quantitatively the same shape with plane-wave pseudopotential

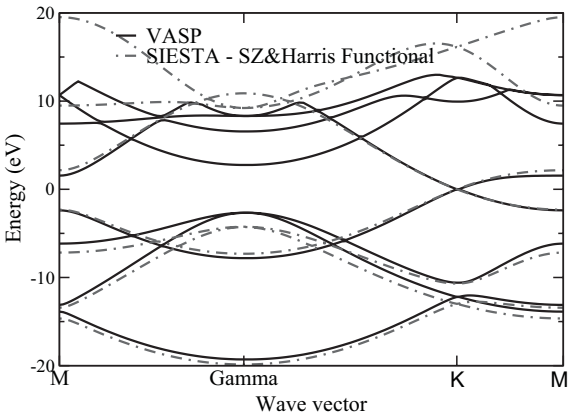

Figure 1 (online color at: www.pss-b.com) Band structure of graphene. The result of VASP is given by solid line. In SIESTA, the dash-dotted line represents the result of SZ basis with Harris functional.

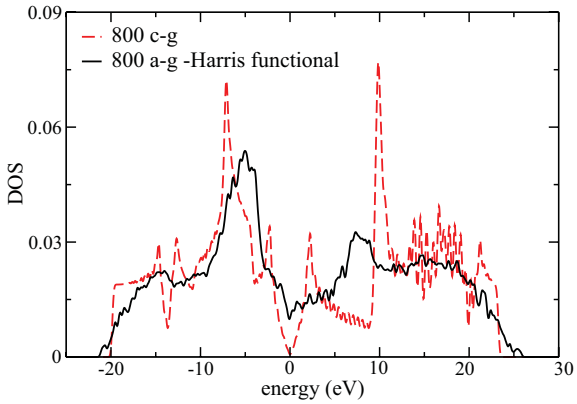

Figure 2 (online color at: www.pss-b.com) Density of states of 800-atom amorphous and crystalline graphene, the Fermi energy is 0 eV. Solid line shows the result of 800 a-g model using Harris functional approximation by SIESTA. The density of states of 800 c-g model is shown by the dashed line, at the Γ point of the Brillouin zone (BZ). The ringing in the crystal is due to incomplete BZ sampling.

calculation (VASP) for the four occupied low-energy bands, unlike the unoccupied higher energy range, where the agreement is rather poor. Machon et al. [6] has shown the SIESTA and VASP calculations are closer if the energy cutoff has been carefully chosen to minimize the total energy.

Also, extensive calculations about vacancy, interstitial defects and doping in crystalline graphene have been undertaken using SIESTA with SZ basis and Harris functional. The results, which will be reported elsewhere, are in good agreement with published experiments and calculations [7, 10–14].

Computationally speaking, VASP is more time-consuming than SIESTA, particularly for large amorphous graphene models we discuss later. For computing total energies and forces, e.g., utilizing quantities soley from the occupied electronic subspace, SIESTA in SZ approximation with Harris functional is a reasonable choice.

4 Amorphous graphene

The three amorphous graphene models are prepared by introducing Stone-Wales defects into a perfect honeycomb lattice with varying concentrations of 5, 6, and 7-member rings.

4.1 Density of states

The electronic density of states for the initial planar 800 a-g model is compared to a Γ point density of states for the crystalline 800 c-g model in Fig. 2 using SIESTA. From this figure, we observe that the electronic structure of the 800 a-g model is vastly different from the crystalline graphene near the Fermi level, as first reported by Kapko et al. [2]. We have constructed additional models with periodic boundary conditions and 836 atoms each (836 a-g1 and 836 a-g2 models). The ring statistics of these three models are given in Table 1 and these show some small differences.

4.2 Loss of planar symmetry

In all three amorphous graphene models, we introduced small random fluctuations in the coordinates, in the direction normal to the graphene plane, and then relaxed with the Harris functional and a SZ basis set. Starting with a flat sheet, the planar symmetry breaks with curvature above or below initial the plane. The final distortion depends on the initial conditions. However, a consistent theme emerges of pentagons inducing curvature as we describe below.

As shown in Tables 2–4, first we randomly moved the atoms along normal direction in the range of $[-\delta r, +\delta r]$, as

Table 1 Ring statistics of 800 a-g, 836 a-g1, and 836 a-g2 models, shown as %.

ring size	800 a-g	836 a-g1	836 a-g2
5	33.5	25	24
6	38	53	52
7	24	19	24
8	4.5	3	0

Table 2 The influence of δr on 800 a-g system relative to initial flat model.

δr (Å)	$\overline{\delta r'}$ (Å)	E_{tot}/N_{atom} (eV)
0.01	0.520	−0.107
0.05	0.525	−0.107
0.07	0.526	−0.107

Table 3 The influence of δr on 836 a-g1 system relative to initial flat model.

δr (Å)	$\overline{\delta r'}$ (Å)	E_{tot}/N_{atom} (eV)
0.01	0.003	0.0
0.05	1.402	−0.102
0.07	1.401	−0.102

Table 4 The influence of δr on 836 a-g2 system relative to initial flat model.

δr (Å)	$\overline{\delta r'}$ (Å)	E_{tot}/N_{atom} (eV)
0.01	0.003	0.0
0.05	1.183	−0.090
0.07	1.180	−0.090

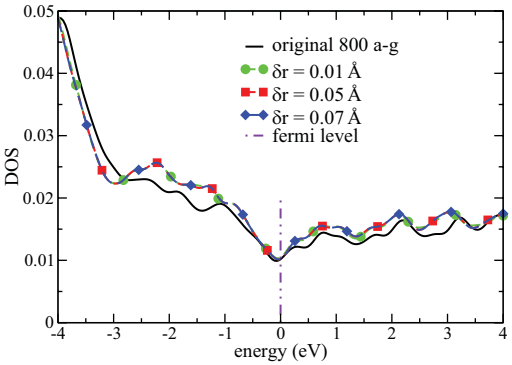

Figure 3 (online color at: www.pss-b.com) Density of states of the original and relaxed puckered system. The solid line is the density of states of original 800-atom amorphous graphene model. The density of states of puckered systems are shown as marked in the plot. The Fermi level is corrected to 0 eV in the plot, as shown in dot-slash line. Additional data are given in Table 1.

shown in the first column of these tables; and the results of relaxing by SIESTA in SZ basis are shown in the second, third, and fourth columns. The prime symbol refers to the relaxed model. Taking the 800-atom a-g model as an example, the influence of puckering the system on the density of states around Fermi level is shown in Fig. 3; a view of the symmetry breaking after relaxing is shown in Figs. 4 and 5 when $\delta r = 0.05$ Å. After breaking the planar symmetry by a tiny amount, say $\delta r = 0.05$ Å, all three models pucker and form the rippled or undulated structure as shown in Figs. 4 and 5.

The radial distribution function $g(r)$ is shown in Fig. 6. From this plot, the mean bond length of the puckered relaxed systems with different initial δr remain near 1.42 Å, the change in ring statistics after relaxing is also not significant. And according to Fig. 4, only one bond broke after relaxation. This implies that the minor difference between the original amorphous graphene model and the relaxed ones is due to these undulations or puckering. This means that diffraction experiments and the associated radial distribution are not a good way to detect puckering and direct imaging will be necessary.

To compare with the puckering of the 800 a-g model, we also introduced the same planar symmetry breaking into a 800 c-g model and relaxed it. As expected, the atoms in this crystalline system maintained planar symmetry. Also we relaxed one of the puckered state (1) to 0 Pa with variable lattice vectors and (2) without periodic boundary condition.

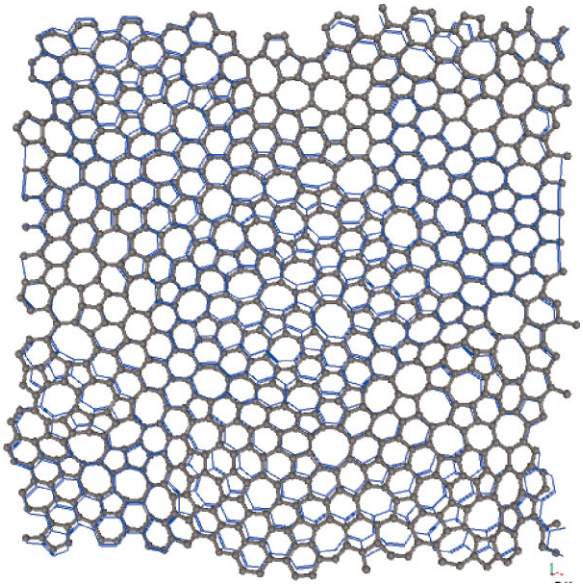

Figure 4 (online color at: www.pss-b.com) The flat view of the relaxed 836 a-g1 system (in gray). The blue background illustrates the original 836 a-g1 model.

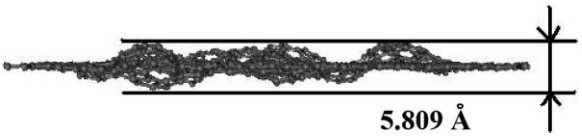

Figure 5 The side view of the relaxed 800 a-g system. The biggest separation along normal direction is marked in the plot.

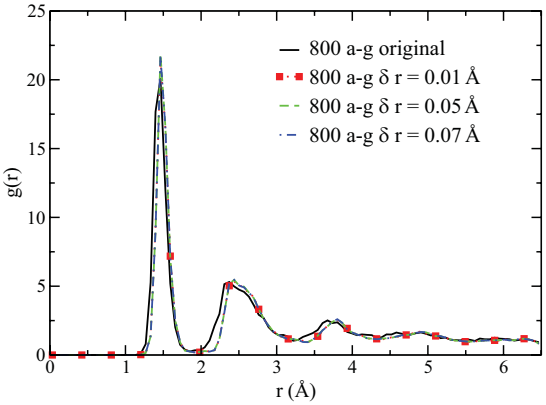

Figure 6 (online color at: www.pss-b.com) Radial distribution function of original flat and puckered 800 a-g system. Additional parameters are given in Table 2.

Within both of these processes some voids arise but the puckered states persist.

In order to find the relation between the ripples in the relaxed systems and the initial random distortion, we tested different seeds in the random number generator (RNG) and also different RNG. The results reveal that changing the seeds or employing different RNG lead to small changes:

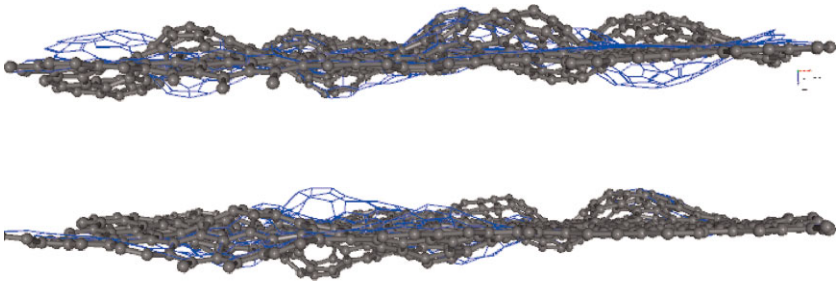

Figure 7 The side view of the final configuration by using new and original RNG. The gray balls and sticks show the result of new RNG. The blue frames represent the result of original RNG.

Figure 8 (online color at: www.pss-b.com) The side view of the final configuration with $\delta r = 0.05$ Å of only moved atoms within pentagons and the original relaxation (distort all atoms). The gray balls and sticks show the result of moving atoms within pentagons. The blue frames represent the result of original distortion.

The maximum mean distortion from the original flat plane ($\overline{\delta r'}$) is about 0.545 Å and the maximum change in total energy compared with original puckered states is around 0.1 eV per atom. Figure 7 shows the side view of the final configurations by using new and original RNG when $\delta r = 0.05$ Å, we can tell that the rippled regions are similar, except certain regions have formed "bucky domes" on opposite sides of the initial plane. These domes can be either be above or below the plane and have a pentagon at the center surrounded by mainly hexagons.

To further test the relation between the ripples and the initial distortion, instead of randomly moving all the atoms of 800 a-g, we only distorted the atoms within pentagons and compared with atoms not included in pentagons. Figure 8 shows the side view of the final configuration of relaxed 800 a-g system when the $\delta r = 0.01$ Å and only the atoms within pentagons were randomly moved. These results are similar to the previous test: (a) The maximum change in $\overline{\delta r'}$ is around 0.625 Å and the maximum change in total energy is around 0.02 eV per atom. (b) No matter which atoms were distorted initially, the final puckered regions involve the same atoms, but possibly puckered in the opposite direction relative to the symmetry plane. Finally, we note that a 128-atom amorphous graphene model made with "melt quenching" [15] exhibits regions puckered around pentagons in a similar fashion to what we report here.

Different initial symmetry breaking leads to different nearly degenerate states after relaxing. However, as stated above, no matter how different the initial condition is (or how different these degenerated state is), the regions that pucker are almost the same. It is evident that different rings induce these ripples. With this motivation, we searched for regions

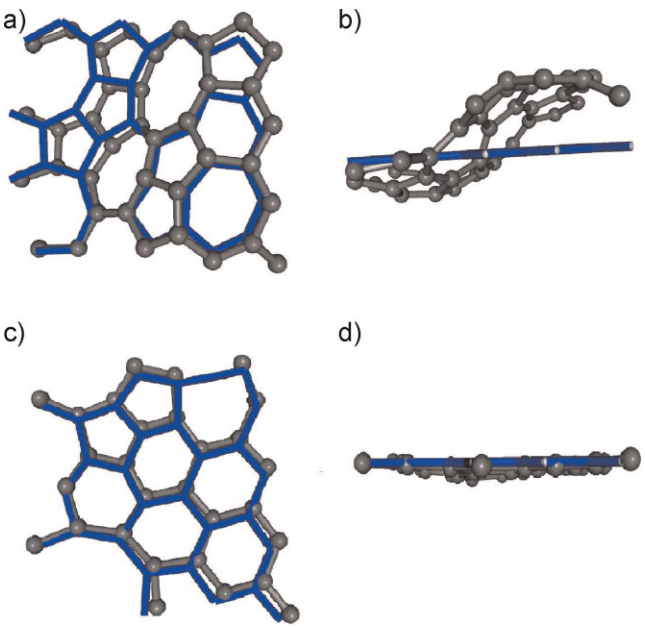

Figure 9 (online color at: www.pss-b.com) The enlarged plot of crinkled and smooth region of 800 a-g model. (a) The top view of the crinkled region. (b) The side view of the crinkled region. (c) The top view of the smooth region. (d) The side view of the smooth region.

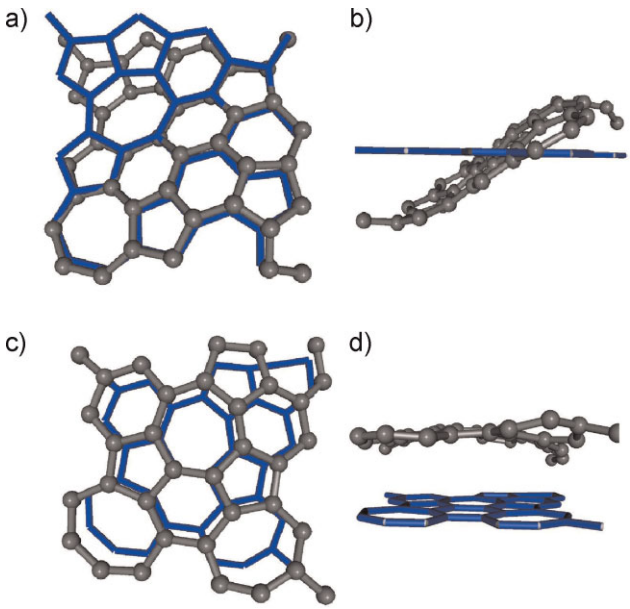

Figure 10 (online color at: www.pss-b.com) The enlarged plot of crinkled and smooth region of 836 a-g1 model. (a) The top view of the crinkled region. (b) The side view of the crinkled region. (c) The top view of the smooth region. (d) The side view of the smooth region.

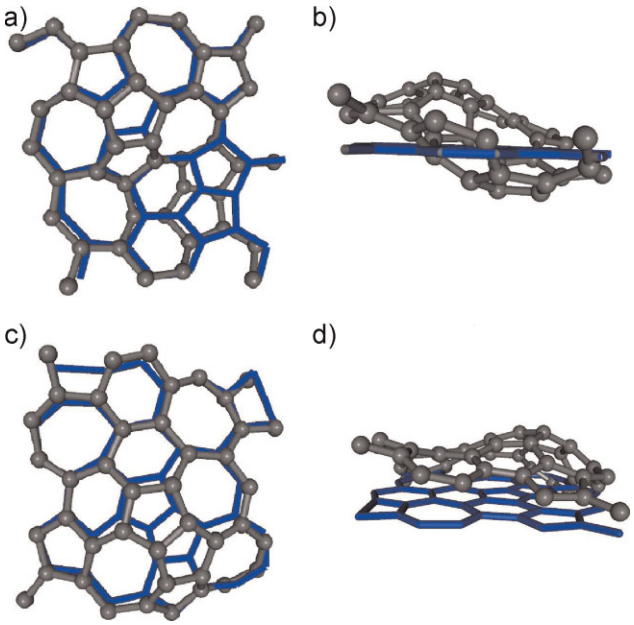

Figure 11 (online color at: www.pss-b.com) The enlarged plot of crinkled and smooth region of 836 a-g2 model. (a) The top view of the crinkled region. (b) The side view of the crinkled region. (c) The top view of the smooth region. (d) The side view of the smooth region.

where the height differences of two neighbor atoms are the largest and smallest in the model (crinkled and smooth regions), as shown in Figs. 9–11. In these plots, the gray atoms are the configuration of crinkled system, and the blue straight lines represent the original model.

As illustrated in Figs. 9 and 10, the puckered areas are the ones with a higher ratio of pentagons to heptagons. The bonds with most distortion do not belong to these pentagons, instead they are within the hexagons or heptagons connecting two pentagons. And the flat areas have fewer pentagons than the puckered areas, and most parts of the flat areas contain hexagons and pentagons. These ripples formed by pentagons strongly remind us of the fullerenes, especially the buckyball (C_{60}) which only contains pentagons and hexagons. The distance from the top to the bottom of the ripples for 800 a-g is around 5.809 Å as shown in Fig. 5, which is comparable to the diameter of buckyball, 6.636 Å. As shown in Figs. 9–11, the crinkled regions are all associated with pentagons.

5 Conclusion We have shown that CRN models of amorphous graphene can pucker and this puckering is associated with pentagonal rings. While the planar conformation is locally stable, a lower energy solution is obtained that is puckered with local maxima and minima in the vicinity of pentagons. The relaxation is performed using a density functional calculation of the electronic energy. The scale of the puckering is consistent with the curvature found in buckyball caps with a pentagon surrounded by larger rings. While we have demonstrated that a well defined puckered state exits, further study is needed to determine whether the puckered state is a single minimum, or rather a series of roughly degenerate local minima with properties akin to the glassy state.

Acknowledgements We want to thank Dr. Mingliang Zhang, Bin Cai and Binay Prasai at Ohio University, Dr. Vitaliy Kapko at Arizona State University and Dr. Mark Wilson at the University of Oxford. The calculations of radial distribution function are done by ISAACS [16]. This work is supported by NSF Grant No. DMR 09-03225 and DMR 07-03973.

References

[1] W. H. Zachariasen, J. Am. Chem. Soc. **54**, 3841 (1932).
[2] V. Kapko, D. A. Drabold, and M. F. Thorpe, Phys. Status Solidi B **247**, 1197–1200 (2010).
[3] S. Reich, J. Maultzsch, and C. Thomsen, Phys. Rev. B **66**, 035412 (2002).
[4] K. V. Christ and H. R. Sadeghpour, Phys. Rev. B **75**, 195418 (2007).
[5] G. Gui, J. Li, and J. Zhong, Phys. Rev. B **78**, 075435 (2008).
[6] M. Machon, S. Reich, C. Thomsen, D. Sanchez-Portal, and P. Ordejon, Phys. Rev. B **66**, 155410 (2002).
[7] S. Yu, W. Zheng, and Q. Jiang, IEEE Trans. Nanotechnol. **9**, 78–81 (2010).
[8] E. Artacho, E. Anglada, O. Dieguez, J. D. Gale, A. Garcia, J. Junquera, R. M. Martin, P. Ordejon, J. M. Pruneda, D. Sanchez-Portal, and J. M. Soler, J. Phys.: Condens. Matter **20**, 064208 (2008).
[9] G. Kresse and J. Furthmuller, Phys. Rev. B **54**, 11169, (1996).
[10] A. Hashimoto, K. Suenaga, A. Gloter, K. Urita, and S. Iijima, Nature **430**, 870–873 (2004).
[11] A. A. El-Barbary, R. H. Telling, C. P. Ewels, M. I. Heggie, and P. R. Briddon, Phys. Rev. B **68**, 144107 (2003).
[12] J. R. Hahn and H. Kang, Phys. Rev. B **60**, 6007 (1999).
[13] A. H. Castro Neto, F. Guinea, N. M. R. Peres, K. S. Novoselov, and A. K. Geim, Rev. Mod. Phys. **81**, 109 (2009).
[14] K. Goetzke and H. J. Klein, J. Non-Cryst. Solids **127**, 215–220 (1991).
[15] D. A. Drabold, Eur. Phys. J. B **68**, 1 (2009).
[16] S. L. Roux and V. Petkov, J. Appl. Crystallogr. **43**, 181–185 (2010).

